

RESEARCH ARTICLE

Investigation of discriminant metabolites in tamoxifen-resistant and choline kinase-alpha-downregulated breast cancer cells using ¹H-nuclear magnetic resonance spectroscopy

Hoe Suk Kim¹, Lianji Tian^{1,2}, Hyeonjin Kim^{1*}, Woo Kyung Moon^{1,2*}

1 Department of Radiology, Seoul National University Hospital, Jongno-gu, Seoul, Korea, **2** Department of Biomedical Science, College of Medicine Seoul National University, Jongno-gu, Seoul, Korea

* hyeonjinkim@snu.ac.kr (HK); moonwk@snu.ac.kr (WKM)



OPEN ACCESS

Citation: Kim HS, Tian L, Kim H, Moon WK (2017) Investigation of discriminant metabolites in tamoxifen-resistant and choline kinase-alpha-downregulated breast cancer cells using ¹H-nuclear magnetic resonance spectroscopy. PLoS ONE 12(6): e0179773. <https://doi.org/10.1371/journal.pone.0179773>

Editor: Aamir Ahmad, University of South Alabama Mitchell Cancer Institute, UNITED STATES

Received: January 5, 2017

Accepted: June 2, 2017

Published: June 23, 2017

Copyright: ©2017 Kim et al. This is an open access article distributed under the terms of the [Creative Commons Attribution License](https://creativecommons.org/licenses/by/4.0/), which permits unrestricted use, distribution, and reproduction in any medium, provided the original author and source are credited.

Data Availability Statement: Data are available within the Dryad Digital Repository (<http://dx.doi.org/10.5061/dryad.64f8c>).

Funding: This work was supported by grant no. 04-2013-1040 and 04-2015-0870 from the SNUH Research Fund to (HSK), and the National Research Foundation of Korea (NRF) grant funded by the Korean government (MEST) (2015R1A2A1A05001860) to (WKM), and (LT) is awardee of graduate student fellowship funded by

Abstract

Metabolites linked to changes in choline kinase- α (CK- α) expression and drug resistance, which contribute to survival and autophagy mechanisms, are attractive targets for breast cancer therapies. We previously reported that autophagy played a causative role in driving tamoxifen (TAM) resistance of breast cancer cells (BCCs) and was also promoted by CK- α knockdown, resulting in the survival of TAM-resistant BCCs. There is no comparative study yet about the metabolites resulting from BCCs with TAM-resistance and CK- α knockdown. Therefore, the aim of this study was to explore the discriminant metabolic biomarkers responsible for TAM resistance as well as CK- α expression, which might be linked with autophagy through a protective role. A total of 33 intracellular metabolites, including a range of amino acids, energy metabolism-related molecules and others from cell extracts of the parental cells (MCF-7), TAM-resistant cells (MCF-7/TAM) and CK- α knockdown cells (MCF-7/shCK- α , MCF-7/TAM/shCK- α) were analyzed by proton nuclear magnetic resonance spectroscopy (¹H-NMRS). Principal component analysis (PCA) and partial least square discriminant analysis (PLS-DA) revealed the existence of differences in the intracellular metabolites to separate the 4 groups: MCF-7 cells, MCF-7/TAM cells, MCF-7-shCK- α cells, and MCF-7/TAM/shCK- α cells. The metabolites with VIP>1 contributed most to the differentiation of the cell groups, and they included fumarate, UA (unknown A), lactate, myo-inositol, glycine, phosphocholine, UE (unknown E), glutamine, formate, and AXP (AMP/ADP/ATP). Our results suggest that these altered metabolites would be promising metabolic biomarkers for a targeted therapeutic strategy in BCCs that exhibit TAM-resistance and aberrant CK- α expression, which triggers a survival and drug resistance mechanism.

Introduction

Recent advancements in high-throughput technologies, such as nuclear magnetic resonance spectroscopy (NMRS), to obtain cancer-associated metabolites have made a significant

Brain Korea 21 Plus (BK21 Plus). The funders had no role in study design, data collection and analysis, decision to publish, or preparation of the manuscript.

Competing interests: The authors have declared that no competing interests exist.

contribution to the understanding of cancer properties related to tumor malignancy and response to therapy. Cellular metabolic alterations driven by genetic and environmental factors, have long been known to be associated with the etiology of cancer [1, 2]. Furthermore, metabolites reflect the drug response or resistance of cancer cells, which is currently one of the most important challenges for cancer treatment [3].

Tamoxifen (TAM), which is an antagonist of the estrogen receptor (ER), is one of the most widely used medications for patients with ER-positive breast cancer (BC). Nonetheless, approximately 30% of ER-positive BCs do not respond to the TAM treatment [4]. TAM-resistant breast cancer cells (BCCs) are the primary cause of tumor recurrence and metastasis, and this resistance is one of the major obstacles for treatment of ER-positive BCs [4–6]. TAM treatment results in a higher content of phosphocholine [7, 8], which may therefore be a reflection of the alteration of cellular metabolism, including choline cancer metabolism in TAM-resistant cells. While mechanisms underlying the metabolic alterations associated with TAM-resistance have yet to be characterized, it is well known that increased choline kinase- α (CK- α) gives rise to an aberrant choline phospholipid metabolism that is associated with drug resistance as well as the aggressiveness of BCCs [9–12]. Therefore, regulation of aberrant CK- α expression may potentially provide an opportunity to characterize metabolites associated with TAM-resistance, which may be valuable for the advancement of diagnostic and therapeutic strategies for TAM-resistant BCCs [13, 14]. On the other hand, autophagy, which is an essential function for regulating cellular metabolic capabilities, has become an attractive target for cancer therapy because it likely contributes to treatment resistance, dormancy and survival of cancer cells [15–17]. In BCCs, autophagy as a protective and survival mechanism can trigger TAM resistance [15, 18].

Unfortunately, there are still no approved therapies available for clinical use that specifically target TAM-resistant BC. New targeted biomarkers are needed to improve the prognosis for TAM-resistant BC patients. Recently, we reported that CK- α knockdown promoted autophagy induction for survival and dormancy of TAM-resistant and CK- α -knockdown BCCs [19]. Therefore, the discriminant metabolites altered by CK- α knockdown and TAM resistance may allow us to understand the properties of breast cancer cells related to promoting autophagy and TAM resistance. There is no comparative study yet of the analysis of altered metabolites resulting from BCCs with TAM-resistance and CK- α knockdown. In this study, we characterize metabolites that may potentially be associated with TAM-resistance and aberrant CK- α expression using proton nuclear magnetic resonance ($^1\text{H-NMR}$) in TAM-resistant BCCs.

Materials and methods

Cell culture

The ER-positive human breast cancer cell line, MCF-7, was obtained from ATCC (Manassas, VA, USA). The TAM-resistant ER-positive human breast cancer cell line, MCF-7/TAM, was kindly provided by professor Sang-kyu Ye (Department of pharmacology, Seoul national university college of medicine, Seoul, Korea). All these cell lines were cultured in Dulbecco's Modified Eagle's Media (DMEM) (WelGENE, Daegu, Korea) containing 10% fetal bovine serum, 100 units/ml penicillin, and 100 $\mu\text{g/ml}$ streptomycin. MCF-7/TAM cells were cultured in medium supplemented with 3 $\mu\text{mol/L}$ TAM (Sigma, St. Louis, MO, USA). All cells were incubated at 37°C in a humidified atmosphere of 95% air/5% CO₂.

Lentiviral vector infection experiments

The lentiviral vector that carries the transgenes for a CK- α specific shRNA and green fluorescent protein (GFP) was purchased from Thermo Scientific (no. RHS4531). The 293T cells

were transfected with a CK- α shRNA lentiviral vector (pLenti-CK- α shRNA), a packing vector (pCMV-dR8.2) and an envelope vector (pCMV-VSVG) using lipofectamine 2000 (Invitrogen, Carlsbad, CA, USA) for lentivirus packaging. Forty-eight hours later, the virus-containing supernatant medium was collected, filtered, and concentrated by ultracentrifugation. In brief, 1×10^5 MCF-7 and MCF-7/TAM cells were seeded in a six-well plate and infected with lentivirus for 6 hours, and after replacing the culture medium, the cells were incubated for an additional 72 hours. The GFP-expressing cells were separated by a FACSCalibur flow cytometer (BD Biosciences, Franklin Lakes, NJ, USA) equipped with a 530-nm filter (bandwidth, ± 15 nm) and a 585-nm filter (bandwidth, ± 21 nm) then analyzed using CellQuest software (BD Biosciences). The downregulation of CK- α in transduced cells was evaluated by RT-PCR and Western blot. The specific CK- α knockdown cells for MCF-7 and MCF-7/TAM were denoted as MCF-7/shCK- α and MCF-7/TAM/shCK- α , respectively.

RNA isolation, cDNA synthesis, and real-time RT-PCR

To evaluate the expression levels of CK- α and CK- β in BCCs, real-time RT-PCR was performed. Briefly, total RNA was extracted from cultured cells using TRIzol reagent (Invitrogen, Carlsbad, CA, USA), and the RNA quantity and quality were determined using a NanoDrop spectrophotometer (Thermo Fisher Scientific Inc. Waltham, MA USA). The cDNA was produced using SuperScript II reverse transcriptase (Invitrogen). Real-time PCR assays were run on an ABI PRISM[®] 7900 using SYBR Green PCR master mix (Applied Biosystems, Foster City, CA, USA). The results were analyzed using the Δ Ct method, which reflected the difference in threshold for the target gene relative to the β -actin in each sample. The following primers were used: CK- α , 5'-CTTGGTGATGAGCCTCGGAA-3', and 5'-AAGTGACCTCTCTGCCGAGAA-3'; CK- β , 5'-AGTCTCGGTTCCAGTTCTAC-3', and 5'-CTTCTGCTCGTTGTTCTCC-3'; β -actin, 5'-CCAACCGCGAGAAGATGACC-3' and 5'-GGAGTCCATCACGATGCCAG-3'.

Western blot

The cells were lysed in RIPA buffer containing a protease inhibitor cocktail (Sigma, St. Louis, MO, USA). The proteins were separated through sodium dodecyl sulfate polyacrylamide gel electrophoresis (SDS-PAGE) and transferred to nitrocellulose membranes. The membranes were blocked with 5% skim milk in Tris-buffered saline and incubated with a primary anti-CK- α antibody (Proteintech Group, Inc., Chicago, IL, USA) and β -actin antibody (Sigma) overnight at 4°C, followed by incubation with horseradish peroxidase-conjugated secondary antibody (Santa Cruz Biotechnology, Santa Cruz, CA, USA) at room temperature for 30 minutes. The blots were developed using enhanced chemiluminescence reagents (Amersham Biosciences, Piscataway, NJ, USA). The relative intensity of the bands observed by Western blotting was analyzed using ImageJ.

Mitochondrial staining with MitoTracker CMXRos

Functional mitochondria were labeled with the mitochondria-specific red-fluorescent dye Mitotracker Red CMXRos (Molecular Probes, Eugene, OR). In brief, cells were treated with 100 nM Mitotracker Red for 10 min, fixed with 2% paraformaldehyde and counterstained with 4',6'-diamidino-2-phenylindole. Mitotracker Red fluorescence was detected using a fluorescence microscope (Leica, Wetzlar, Germany). A total of 1.0×10^6 cells were pelleted and suspended in 1 ml of pre-warmed complete medium with a final concentration of 100 nM Mitotracker Red for 10 min at 37°C. Excess dye was removed with 2 washes in pre-warmed complete medium at 37°C and the mean fluorescence intensity (MFI) value in Mitotracker Red-labeled cells was analyzed using flow cytometry (Becton Dickinson).

$^1\text{H-NMR}$

MCF-7, MCF-7/TAM, MCF-7/shCK- α , and MCF-7/TAM/shCK- α cells were harvested, collected as cell pellets containing 3×10^7 cells per sample, and stored at -80°C until the onset of $^1\text{H-NMR}$ data acquisition. In brief, frozen cell pellets were thawed with D_2O made in PBS, mixed with 1.5 mM sodium 3-(trimethylsilyl)-propionate-2,2,3,3- d_4 (TSP; Cambridge Isotope Laboratories, Inc., Andover, MA) as an internal standard, centrifuged to remove precipitates, and then placed immediately on ice until the onset of data acquisition. One-dimensional $^1\text{H-NMR}$ spectra were acquired on a Bruker Avance 600 system (14.1 T) equipped with 5-mm TXI cryoprobe spectrometers (Bruker BioSpin Corp. Ettlingen, Germany). Spectra were acquired using a CPMG sequence at $20^\circ\text{C} \pm 1$ with the following sequence parameters: flip angle = $90^\circ/180^\circ$, fixed echo time = 1 ms, loop for T2 filter = 20, spectral width = 16 kHz, relaxation delay = 2 s, 32k data points, and 128 scans. NMR spectra were processed using MestReNova (Mestrelab research, Santiago de, Spain) and jMRUI [20]. The time-domain data were apodized with an exponential function (1 Hz) and then Fourier transformed followed by phase- and baseline-correction. The chemical shifts of the peaks were calibrated relative to the TSP signal at 0.00 ppm. The individual metabolites were quantified by estimating the peak areas in the corresponding spectral regions of interest (Table 1), followed by normalization to the measurements for TSP.

Data analysis

The quantitative analysis of the $^1\text{H-NMR}$ spectra was performed on 4–6 samples of MCF-7 ($n = 4$), MCF-7/TAM ($n = 4$), MCF-7/shCK- α ($n = 6$) and MCF-7/TAM/shCK- α ($n = 5$) cells. Given the number of cell groups and $^1\text{H-NMR}$ -detectable metabolites and the potential correlations among the metabolites, a multivariate analysis was performed using SIMCA (v.13; Umetrics Inc., San Jose, CA). Data were first inspected by performing principal components analysis (PCA), followed by partial least-squares discriminant analysis (PLS-DA). Then, a set of $^1\text{H-NMR}$ measures were sorted out according to the variable influence on projection (VIP) values as a measure of the relative discriminatory potential of the individual $^1\text{H-NMR}$ measures [21]. Those $^1\text{H-NMR}$ measures with $\text{VIP} > 1$ were considered to have contributed most to the differentiation of the cell groups, for which further statistical analyses were performed for multiple group comparisons using the Student's t -test and analysis of variance (ANOVA). A p value of < 0.05 was considered to be statistically significant.

Results

Expression of the autophagic maker LC3II in CK- α knockdown and TAM-resistant BCCs

GFP and CK- α shRNA-transduced cells exhibited over 95% expression of GFP (Fig 1A). A fluorescence microscope showed stable overexpression of GFP in MCF-7/shCK- α and MCF-7/TAM/shCK- α (Fig 1B). CK- α mRNA was significantly higher in MCF-7/TAM (1.72 ± 0.16) relative to MCF-7, and the transduction of shRNA led to a significant and specific downregulation of CK- α mRNA in MCF-7/shCK- α (0.40 ± 0.13) and MCF-7/TAM/shCK- α (0.39 ± 0.13) compared to MCF-7 ($***p < 0.001$, $0.001 < **p < 0.05$, Fig 1C). However, the level of CK- β mRNA was not changed in MCF-7/TAM, MCF-7/shCK- α and MCF-7/TAM/shCK- α relative to MCF-7. As shown in Fig 1D, the levels of CK- α protein assessed by Western blot were higher in MCF-7/TAM (1.55 ± 0.07) and decreased in MCF-7/shCK- α (0.68 ± 0.06) and MCF-7/TAM/shCK- α (0.55 ± 0.17) compared to MCF-7 ($*p < 0.05$, $0.001 < **p < 0.05$, $*** > p$). As expected, ER- α expression decreased in MCF-7/TAM (0.35 ± 0.12) and MCF-7/TAM/shCK- α

Table 1. Assignment of metabolites observed by $^1\text{H-NMR}$ in cancer cell lysates.

Metabolites	$^1\text{H-NMR}$ chemical shift (ppm)
Leucine	1.090–0.810
Isoleucine	1.090–0.810
Valine	1.090–0.810
Alanine	1.499–1.470
Glutarate	1.870–1.850
Acetate	1.957–1.874
N-acetyl-aspartate	2.098–1.968
N-acetyl-amino acid	2.098–1.968
Glutamate	2.379–2.331
Succinate	2.416–2.402
Glutamine	2.496–2.417
Glutathione	2.601–2.525
Creatine	3.052–3.036
Choline	3.215–3.206
Phosphocholine	3.233–3.220
Glycerophosphocholine	3.245–3.233
Taurine	3.456–3.396
Myo-inositol	3.552–3.503
Glycine	3.570–3.552
Lactate	4.105–4.095
Threonine	4.250–4.240
Maleate	6.022–5.957
Fumarate	6.529–6.516
Tyrosine	7.217–7.180
Phenylalanine	7.460–7.409
Histidine	7.888–7.869
Formate	8.443–8.430
AXP	6.022–5.957
UXP	6.022–5.957
NAD	9.161–9.126
unknown A	1.159–1.130
unknown C	5.574–5.538
unknown E	8.620–8.600

<https://doi.org/10.1371/journal.pone.0179773.t001>

(0.28 ± 0.08) ($***p < 0.001$, Fig 1E). LC3II was used as a reliable autophagosome marker for monitoring autophagy and was increased in MCF-7/shCK- α (1.66 ± 0.65), MCF-7/TAM (1.64 ± 0.44) and MCF-7/TAM/shCK- α (2.48 ± 0.31) compared to the parental MCF-7 ($*p < 0.05$, $0.001 < **p < 0.05$, Fig 1F).

Only a few caspase-3-positive cells were observed in MCF-7/shCK- α . However, shRNA-mediated partial CK- α knockdown was not sufficient to render apoptotic cell death and decreased cell proliferation activity in MCF-7/TAM/shCK- α (S1 Fig). We evaluated the mitochondrial dysfunction in cells loaded with MitoTracker CMXRos to examine changes in either mitochondrial mass, membrane potential, or both. Fluorescence microscopy of MCF-7/shCK- α and MCF-7/TAM/shCK- α revealed that selective mitochondria staining using MitoTracker CMXRos decreased through CK- α knockdown (S2 Fig). The mean fluorescence intensity (MIF) of MitoTracker CMXRos was significantly lower in MCF-7/shCK- α and MCF-7/TAM/

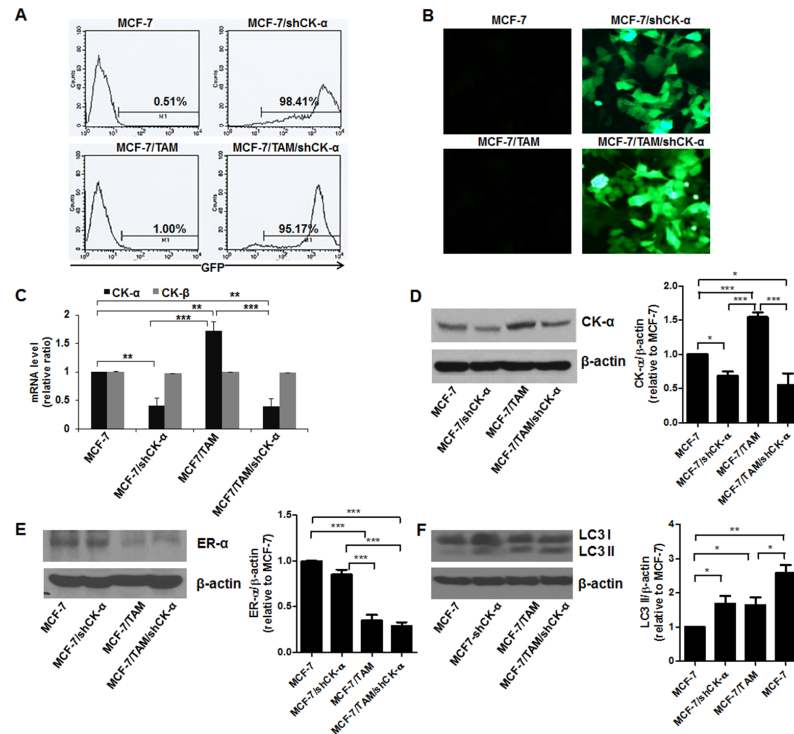


Fig 1. Analysis of choline kinase- α (CK- α), estrogen receptor- and LC3 in CK- α -knockdown cells in MCF-7 and MCF-7/TAM. (A) Flow cytometric analysis of GFP positive cells in MCF-7/shCK- α and MCF-7/TAM/shCK- α transduced with lentivirus containing CK- α shRNA and GFP. (B) Images of GFP expression in MCF-7/shCK- α and MCF-7/TAM/shCK- α . (C) RT-PCR analysis of CK- α and CK- β in MCF-7, MCF-7/TAM, MCF-7/shCK- α and MCF-7/TAM/shCK- α . (D) Western blot analysis of CK- α in MCF-7, MCF-7/TAM, MCF-7/shCK- α and MCF-7/TAM/shCK- α . (E) Western blot analysis of ER- α in MCF-7, MCF-7/TAM, MCF-7/shCK- α and MCF-7/TAM/shCK- α . (F) Western blot analysis of LC3I/II in MCF-7, MCF-7/TAM, MCF-7/shCK- α and MCF-7/TAM/shCK- α . Data are presented as the mean \pm standard error. * p <0.05, 0.001<** p <0.05, *** p <0.001.

<https://doi.org/10.1371/journal.pone.0179773.g001>

shCK- α , and the intensity was significantly higher in MCF-7/TAM, which suggests there were changes in mitochondrial mass and mitochondrial membrane potential (S2 Fig).

Analysis of metabolites by $^1\text{H-NMR}$ in CK- α knockdown and TAM-resistant BCCs

The $^1\text{H-NMR}$ spectra of the samples from MCF-7 (MC), MCF-7/TAM (MT), MCF-7/shCK- α (Msh) and MCF-7/TAM/shCK- α (MTsh) showed a wide variety of metabolite resonances. A total of 30 metabolites were identified, which included amino acids, energy metabolism-related molecules (e.g., pyruvate, succinate, lactate, creatine), and others (cholines, amines, amides, nucleotides, etc.). There were also 3 unidentified resonances (Table 1).

In the PCA analysis, the MCF-7 (MC), MCF-7/TAM (MT), MCF-7/shCK- α (Msh) and MCF-7/TAM/shCK- α (MTsh) groups were well separated from each other without potential outliers (Fig 2A). In the PLS-DA analysis, the cell groups were well differentiated among each other (Fig 2B). The score plot (Fig 2B) also showed effective differentiation of the cell types according to TAM-resistance ((MCF-7(MC) and MCF-7/shCK- α (Msh) vs. MCF-7/TAM(MT) and MCF-7/TAM/shCK- α (MTsh)) and CK- α knockdown ((MCF-7 (MC) and MCF-7/TAM(MT) vs. MCF-7/shCK- α (Msh) and MCF-7/TAM/shCK- α (MTsh)). According

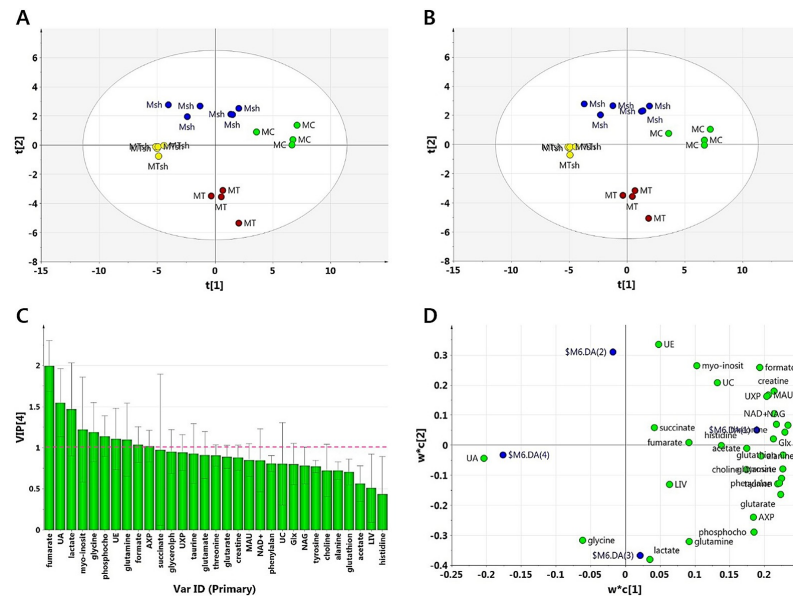


Fig 2. PCA and PLS-DA for MCF-7, MCF-7/shCK- α , MCF-7/TAM and MCF-7/TAM/shCK- α groups. (A) PCA for the inspection and overview of the data set. (B) Score plot for the investigation of group differentiation among MCF-7 (MC, n = 4, green), MCF-7/shCK- α (Msh, n = 6, blue), MCF-7/TAM (MT, n = 4, red), and MCF-7/TAM/shCK- α (MTsh, n = 5, yellow) cell groups. (C) VIP values as a measure of the discriminatory potential of the individual metabolites in the group differentiation. (UA: unknown resonance A, lactate, UE: unknown resonance E, glutamine, formate, AXP: AMP/ADP/ATP, UXP: UMP/UDP/UTP, MAU: maleate/AXP/UXP, UC: unknown resonance C, NAG: N-acetyl-aspartate/-amino acid/glutamate, Glx: glutamate/glutamine, LIV: leucine/isoleucine/valine). (D) Loading plot showing the relative contribution of the metabolites to the scores in the score plot. By matching the positions in the score plot and loading plot, the correlations between the individual metabolites and the cell groups were determined.

<https://doi.org/10.1371/journal.pone.0179773.g002>

to the loading plot (Fig 2D) in combination with the score plot (Fig 2B), the majority of the metabolites tended to be higher in MCF-7 (MC) than in the rest of the cell groups. The relative contributions of the metabolites to the differentiation of the cell groups are shown in order in Fig 2C. The metabolites with VIP > 1 were fumarate, UA (unknown A), lactate, myo-inositol, glycine, phosphocholine, UE (unknown E), glutamine, formate, and AXP (AMP/ADP/ATP).

Key metabolites altered by CK- α knockdown in TAM-resistant BCCs

Fig 3 shows the results of the t-test between the cell groups for those metabolites (fumarate, UA, lactate, myo-inositol, glycine, phosphocholine, UE, glutamine, formate, and AXP) with VIP > 1. There is a trend towards high concentrations of lactate, glycine, phosphocholine, and glutamine in the MCF-7/TAM with respect to the other three cell groups. The MCF-7/shCK- α had significantly higher myo-inositol concentrations than the other cell groups. The concentrations of formate were negligible in the TAM-resistant cell groups (MCF-7/TAM and MCF-7/TAM/shCK- α). Fumarate was detected only in MCF-7 and MCF-7/TAM/shCK- α . Phosphocholine, glutamine and AXP were remarkably decreased in the CK- α knockdown cell group (MCF-7/shCK- α and MCF-7/TAM/shCK- α). Unknown A was detected only in MCF-7/TAM/shCK- α . Unknown E was not detected in MCF-7/TAM. The results of the t-test for the rest of the metabolites are shown in S1 Fig. Overall, CK- α knockdown and/or TAM-resistance led to decreased metabolite concentrations, including choline-related metabolites (S3 Fig).

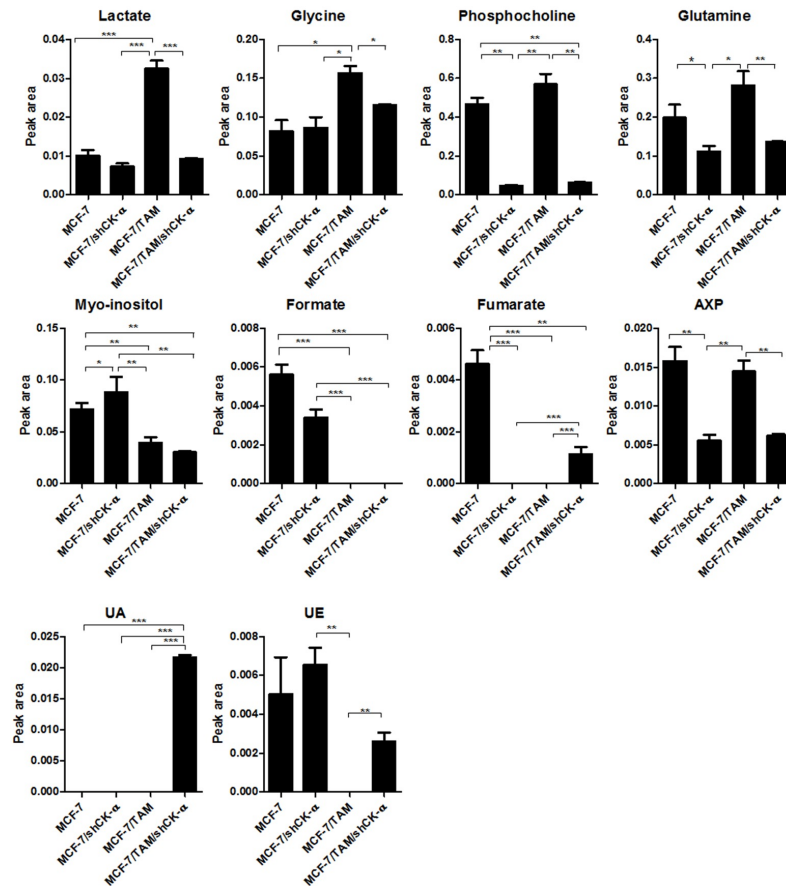


Fig 3. Comparison of the concentrations of the metabolites with VIP>1 among the MCF-7, MCF-7/shCK- α , MCF-7/TAM, and MCF-7/TAM/shCK- α cell groups. Increased lactate, glycine, phosphocholine, glutamine, and succinate in MCF-7/TAM relative to the other cell groups. Increased myo-inositol in MCF-7/shCK- α relative to the other cells. Non-detectable formate in MCF-7/TAM and MCF-7/TAM/shCK- α . Non-detectable fumarate in 7/shCK- α and MCF-7/TAM and MCF-7/TAM/shCK- α . Decreased AXP in MCF-7/shCK- α cells and MCF-7/TAM/shCK- α relative to MCF-7 and MCF-7/TAM. The spectra were normalized against total intensity and averaged over the samples in MCF-7, MCF-7/shCK- α , MCF-7/TAM and MCF-7/TAM/shCK- α . All values are presented as the mean \pm standard error. * $p < 0.05$, ** $0.001 < p < 0.05$, *** $p < 0.001$.

<https://doi.org/10.1371/journal.pone.0179773.g003>

Discussion

Although it has anti-estrogen activity, TAM is widely used to treat ER-positive breast tumors as an adjuvant therapy for early-stage hormone-sensitive breast cancer or first line therapy for metastatic hormone-sensitive breast cancer, and as many as 30% of patients can be refractory to TAM and acquire resistance to TAM along with the loss of ER- α [6, 22–24]. CK- α is one of the targets of therapeutic strategies because it is a key enzyme in choline metabolism and might contribute to TAM resistance [11, 19]. In addition, the metabolic survival-promotion function of autophagy, which is activated in drug resistant BCCs, is also one of the therapeutic targets [19]. Our recent study reported a potential connection between autophagy and CK- α in the mechanisms driving TAM resistance in ER+ BCCs. Interestingly, TAM-resistant and/or CK- α -knockdown BCCs (MCF-7/TAM and MCF-7/TAM/shCK- α) exhibited notable induction of autophagy through accumulation of LC3-II and P62 as well as the suppression of AKT, ERK and mTOR, which can contribute to the protective and survival mechanisms of MCF-

7/TAM and MCF-7/TAM/shCK- α cells [19]. According to the study reported by Sanchez-Lopez *et al* [25], the pharmacological inhibition of CK- α by MN58b and RSM932A changes CK- α protein folding and leads to apoptosis via CHOP-mediated ER stress in cancer cells, including MCF-7, but partial genetic inhibition of CK- α by small interfering RNA (siRNA) does not induce apoptosis. The potent downregulation of endogenous CK- α protein using siRNA in breast cancer cells (MDA-MB-231, MDA-MB-468) and cervical cancer cells (HeLa) reduces proliferation, and results in significant cell death through apoptosis [12, 26, 27]. We rarely observed few caspase-3-stained cells, indicating that there is an apoptotic response in MCF-7/shCK- α but not MCF-7/TAM/shCK- α as well as a reduction of proliferation activity in MCF-7/TAM/shCK- α , suggesting that there is partial downregulation (approximately 30%) of the CK- α proteins in our shRNA system that is not sufficient to render apoptotic cell death but reduces proliferation activity in MCF-7/TAM/shCK- α . The partial knockdown of CK- α protein in our study may limit the reproducibility of previous studies. In addition, these discrepancies with the many previous reports would be due to distinct pharmacokinetic or target selectivity of pharmacological inhibitors as well as different knockdown efficiency of the siRNA or shRNA. When CK- α is inhibited either genetically (shRNA) or pharmacologically (CK37) in our previous study [19], shRNA and CK37 increased the autophagosomal marker LC3-II expression, but rendered differential effects on the expression level of p62, a marker of autophagic flux as shRNA, which suggest that genetic or pharmacological inhibition of CK- α can perturb a biological and metabolic system in different ways. Besides being a competitive CK inhibitor, CK37 suppresses choline uptake [28]. In general, different cellular responses can be triggered by concentration- and time-dependent pharmacokinetics of CK37. Therefore, pharmacological inhibitor should be used with caution. For this reason, the metabolic analysis of CK37-treated cells was not performed in this study. In our study, the lack of correlation between the levels of mRNA and proteins of CK- α was observed in CK- α knockdown cells. This is because protein levels are generally affected by many steps in their synthesis, stability and degradation [29]; cells can control the rates of degradation and synthesis of proteins depending on a number of different conditions, even for those proteins with similar functions. We speculate that the lack of a strong downregulation of the CK- α protein levels in CK- α knockdown cells may be associated with the steps of high stability or low degradation.

We designed the study to depict metabolic differences based on TAM resistance and CK- α expression linked with protective autophagy, which could potentially provide a direction toward targets for validation studies and the development of therapeutics in ER+ BC patients. To the best of our knowledge, this is the first study to apply $^1\text{H-NMR}$ to identify altered metabolites in the total lysate of TAM-resistant and/or CK- α -knockdown BCCs linked with TAM resistance as well as protective autophagy for use as predictors of the hormone and CK- α gene therapy. In the present study, we quantified a total of 33 metabolites (including 3 unknown resonances) in the MCF-7, MCF-7/shCK- α , MCF-7/TAM and MCF-7/TAM/shCK- α cells. In the subsequent multivariate analysis, a statistical model was constructed that effectively differentiated cell types according to TAM-resistance and CK- α expression. The metabolites that contributed most to differentiation were found to be fumarate, UA, lactate, myo-inositol, glycine, phosphocholine, UE, glutamine, formate, and AXP. Increased glycolysis has been linked to drug resistance through increased lactate production [30]. It was also reported very recently that lactate is critical for sustaining protective autophagy in cancer cells, including ovarian carcinoma cells, glioblastoma cells and gastric cancer cells [31, 32]. In addition, elevated lactate is associated with drug resistance and stemness of BCCs, which drives recurrence, metastasis and poor clinical outcomes in BC patients [30, 32, 33]. Glycine provides the essential precursors for the synthesis of proteins, nucleic acids, and lipids, and it is a crucial metabolite for cancer cell proliferation and growth [34–36]. Glutamine participates as a nutrient in energy

formation, redox homeostasis, and macromolecular synthesis and influences the suppression/induction of autophagy through a complex mechanism [37, 38]. High expression and activity of CK- α in BCCs elevates phosphocholine levels, which serves as a biomarker, thus reflecting breast cancer progression, especially in cases of drug resistance [9, 10, 22, 39, 40]. As noted in the results above, the MCF-7/TAM cells exhibiting TAM resistance and protective autophagy had high levels of lactate, glycine, glutamine, and phosphocholine, whereas CK- α knockdown reduced the levels of these metabolites, suggesting that these metabolites could be regulated by CK- α -mediated mechanisms and could serve as biomolecules and energy sources to overcome TAM insult and activate protective autophagy of damaged products. The level of myo-inositol was reported to be higher in MCF-7 and BT-474 cells (luminal A type of breast cancer cell line) than in MDA-MB-468 and MDA-MB-231 cells (triple negative breast cancer cell line), and there was also an increase in paclitaxel [41].

The CK defect causes a decreased phosphatidylcholine (PtdCho) level in the mitochondrial membrane, leading to mitochondrial dysfunction and degradation by autophagy through a process called mitophagy [27, 42]. The measurement of PtdCho requires separate preparation of cells, for instance, cells dissolved in methanol-chloroform solvent, for precise quantification of PtdCho levels from ¹H-NMR spectra [43, 44], which was not available in our study. For this reason, we did not attempt to quantify PtdCho in our samples dissolved in D₂O, which is one of the limitations of our study. Given its importance in the metabolism of BCCs [43, 45], the measurement of PtdCho would have provided additional information in the interpretation of our data. For instance, it might have corroborated the relationships of PtdCho with mitochondrial dysfunction, especially autophagy and drug resistance in both CK- α knockdown cells and TAM-resistant cells.

Interestingly, we found that CK- α knockdown in ER+BCCs led to a decrease in MitoTracker CMXRos-stained mitochondria and the MIF of MitoTracker CMXRos, which indicates that there is mitochondrial dysfunction. In cancer patients, cancer cells with “healthy mitochondria” are actually more resistant to conventional therapies [46]. The treatment with TAM can induce the aggregation of mitochondria and mitochondrial-mediated apoptosis in BCCs [47], but mitochondrial function is improved in TAM-resistant BCCs [48]. In accordance with these findings, we observed that MCF-7/TAM cells exhibited higher levels in mitochondria staining and MIF of MitoTracker CMXRos compared to parent MCF-7 cells and MCF-7/shCK- α and MCF-7/TAM/shCK- α exhibited a loss of mitochondria compared to MCF-7 and MCF-7/TAM. According to a previous study by Rodríguez-González *et al.* [49], a strong CK- α inhibition by MN58b in cervical cancer cells induces cytochrome c release, followed by a loss of mitochondrial potential, which are associated with mitochondria-mediated apoptosis. Our study shows that a partial knockdown of CK- α by shRNA in breast cancer cells preferentially induced mitochondria-mediated autophagy. The different outcomes reported by Rodríguez-González *et al.* may likely be due to stronger inhibition of CK- α activity in their study. Our findings suggest that understanding mitochondrial dysfunction (mitochondria-mediated autophagy or apoptosis) may be the key to unlocking new anticancer therapies and preventing the onset of drug resistance in cancer patients. Additionally, mitochondrial metabolism may be a key target for designing novel anticancer therapies.

The depletion of myo-inositol induces protective autophagy in human cells by influencing both ER and mitochondria [50, 51]. Therefore, the low levels of myo-inositol in TAM-resistant cells (MCF-7/TAM and MCF-7/TAM/shCK- α) might have contributed to the induction of protective autophagy. Some cancer cells exhibit a high rate of formate release when growing in a standard culture medium, and a recent study has shown that electron transport chain dysfunction leads to a reduction in mitochondrial formate production from serine [38]. An excess amount of intracellular fumarate due to mutation or loss of fumarate hydratase is detected in

the majority of primary tumors and metastases, and the involved mechanisms are potentially associated with treatment resistance [52]. Formate and fumarate also have critical roles in regulating epigenetic changes and maintaining cellular redox homeostasis [53]. Of note, formate and fumarate were remarkably decreased by CK- α knockdown and were hardly detected in the MCF-7/TAM cells. Based on the above reports, undetectable formate and fumarate in MCF-7/TAM cells might be associated with excessive activation of fumarate hydratase and dysfunction of the mitochondrial electron transport chain. These results suggest that the fumarate hydratase and mitochondrial electron transport chain could also be the target for TAM-resistance and protective autophagy in ER+ BC patients.

In conclusion, the discriminant metabolites found in TAM-resistant and/or CK- α knockdown BCCs can be used as metabolic markers to predict TAM resistance and aberrant CK- α expression and may represent changes in the metabolic activity of signaling pathways underlying the protective autophagy triggered by TAM resistance and CK- α knockdown. Our findings may provide further insight into the different therapeutic responses of BCCs and additional information about current diagnostic and therapeutic assessments of TAM-resistant BCCs. Further studies on the blood samples or needle biopsies from TAM-resistant BC patients would be required to validate the potential clinical applicability of the metabolic biomarkers found in the BCCs with TAM resistance and aberrant CK- α expression.

Supporting information

S1 Fig. Caspase-3 and Ki-67 staining and cell cycle analysis in MCF-7, MCF-7/shCK- α , MCF-7/TAM and MCF-7/TAM/shCK- α . (A) Immunostaining of activated caspase-3, which indicates apoptotic response. A small amount of caspase-3 staining (white arrow) was observed only in MCF-7/shCK- α . (B) Immunostaining of Ki-67, which indicates proliferative activity. The Ki-67-stained cell population (red arrow) was decreased in MCF-7/shCK- α , MCF-7/TAM and MCF-7/TAM/shCK- α . (C) Cell cycle analysis using flow cytometry with propidium iodide. A decrease in the S phase population and an increase in the G0/G1 phase population were observed in MCF-7/TAM and MCF-7/TAM/shCK- α relative to MCF-7 and MCF-7/shCK- α . An intriguing finding in MCF-7/TAM/shCK- α was a further increase in the G0/G1 phase population and a decrease in the S phase population compared to MCF-7/TAM. (TIF)

S2 Fig. Analysis of mitochondria in MCF-7, MCF-7/shCK- α , MCF-7/TAM and MCF-7/TAM/shCK- α using the mitochondrial dye MitoTracker CMXRos. (A) Fluorescence microscopy and (B) flow cytometry analysis of mitochondrial dye uptake. The MitoTracker CMXRos-stained mitochondria decreased in MCF-7/shCK- α . The mean fluorescence intensity (MIF) of MitoTracker CMXRos was significantly lower in MCF-7/shCK- α and MCF-7/TAM/shCK- α , and it was significantly higher in MCF-7/TAM, which suggests that there is a change in mitochondrial mass or mitochondrial membrane potential compared to the parent MCF-7. Scale bar, 20 μ m. All values are presented as the mean \pm standard error. * $p < 0.05$, ** $0.05 < p < 0.001$, *** $p < 0.001$. (TIF)

S3 Fig. Statistical significance of metabolites analyzed in MCF-7, MCF-7/shCK- α , MCF-7/TAM and MCF-7/TAM/shCK- α . The peak areas were normalized to total signal and averaged across the samples for each individual groups of MCF-7, MCF-7/shCK- α , MCF-7/TAM and MCF-7/TAM/shCK- α . All values are presented as the mean \pm standard error. * $p < 0.05$, ** $0.05 < p < 0.001$, *** $p < 0.001$. (TIF)

Author Contributions

Conceptualization: HSK HK WKM.

Data curation: HSK LT.

Formal analysis: HSK LT HK.

Funding acquisition: HSK WKM.

Methodology: HSK HK.

Project administration: HSK HK WKM.

Resources: HSK LT HK.

Software: LT HK.

Supervision: HSK HK WKM.

Validation: HSK LT HK WKM.

Visualization: HSK LT HK WKM.

Writing – original draft: HSK.

Writing – review & editing: HSK LT HK WKM.

References

1. Sullivan LB, Gui DY, Vander Heiden MG. Altered metabolite levels in cancer: implications for tumour biology and cancer therapy. *Nat Rev Cancer*. 2016; 16(11):680–93. <https://doi.org/10.1038/nrc.2016.85> PMID: 27658530.
2. Griffin JL, Shockcor JP. Metabolic profiles of cancer cells. *Nat Rev Cancer*. 2004; 4(7):551–61. <https://doi.org/10.1038/nrc1390> PMID: 15229480.
3. Rahman M, Hasan MR. Cancer Metabolism and Drug Resistance. *Metabolites*. 2015; 5(4):571–600. <https://doi.org/10.3390/metabo5040571> PMID: 26437434;
4. Riggins RB, Schrecengost RS, Guerrero MS, Bouton AH. Pathways to tamoxifen resistance. *Cancer letters*. 2007; 256(1):1–24. <https://doi.org/10.1016/j.canlet.2007.03.016> PMID: 17475399;
5. Shou J, Massarweh S, Osborne CK, Wakeling AE, Ali S, Weiss H, et al. Mechanisms of tamoxifen resistance: increased estrogen receptor-HER2/neu cross-talk in ER/HER2-positive breast cancer. *Journal of the National Cancer Institute*. 2004; 96(12):926–35. PMID: 15199112.
6. Viedma-Rodriguez R, Baiza-Gutman L, Salamanca-Gomez F, Diaz-Zaragoza M, Martinez-Hernandez G, Ruiz Esparza-Garrido R, et al. Mechanisms associated with resistance to tamoxifen in estrogen receptor-positive breast cancer (review). *Oncology reports*. 2014; 32(1):3–15. <https://doi.org/10.3892/or.2014.3190> PMID: 24841429.
7. Cabot MC, Zhang Z, Cao H, Lavie Y, Giuliano AE, Han TY, et al. Tamoxifen activates cellular phosphatase C and D and elicits protein kinase C translocation. *International journal of cancer Journal international du cancer*. 1997; 70(5):567–74. PMID: 9052757.
8. Neeman M, Degani H. Metabolic studies of estrogen- and tamoxifen-treated human breast cancer cells by nuclear magnetic resonance spectroscopy. *Cancer research*. 1989; 49(3):589–94. PMID: 2562927.
9. Ramirez de Molina A, Rodriguez-Gonzalez A, Gutierrez R, Martinez-Pineiro L, Sanchez J, Bonilla F, et al. Overexpression of choline kinase is a frequent feature in human tumor-derived cell lines and in lung, prostate, and colorectal human cancers. *Biochemical and biophysical research communications*. 2002; 296(3):580–3. PMID: 12176020.
10. Ramirez de Molina A, Gutierrez R, Ramos MA, Silva JM, Silva J, Bonilla F, et al. Increased choline kinase activity in human breast carcinomas: clinical evidence for a potential novel antitumor strategy. *Oncogene*. 2002; 21(27):4317–22. <https://doi.org/10.1038/sj.onc.1205556> PMID: 12082619.
11. Shah T, Wildes F, Penet MF, Winnard PT Jr., Glunde K, Artemov D, et al. Choline kinase overexpression increases invasiveness and drug resistance of human breast cancer cells. *NMR in biomedicine*. 2010; 23(6):633–42. <https://doi.org/10.1002/nbm.1510> PMID: 20623626;

12. Glunde K, Raman V, Mori N, Bhujwala ZM. RNA interference-mediated choline kinase suppression in breast cancer cells induces differentiation and reduces proliferation. *Cancer research*. 2005; 65(23):11034–43. <https://doi.org/10.1158/0008-5472.CAN-05-1807> PMID: 16322253.
13. Serkova NJ, Niemann CU. Pattern recognition and biomarker validation using quantitative ¹H-NMR-based metabolomics. *Expert review of molecular diagnostics*. 2006; 6(5):717–31. <https://doi.org/10.1586/14737159.6.5.717> PMID: 17009906.
14. Serkova NJ, Spratlin JL, Eckhardt SG. NMR-based metabolomics: translational application and treatment of cancer. *Current opinion in molecular therapeutics*. 2007; 9(6):572–85. PMID: 18041668.
15. Zarzynska JM. The importance of autophagy regulation in breast cancer development and treatment. *Biomed Res Int*. 2014; 2014:710345. <https://doi.org/10.1155/2014/710345> PMID: 25317422;
16. Sui X, Chen R, Wang Z, Huang Z, Kong N, Zhang M, et al. Autophagy and chemotherapy resistance: a promising therapeutic target for cancer treatment. *Cell Death Dis*. 2013; 4:e838. <https://doi.org/10.1038/cddis.2013.350> PMID: 24113172;
17. Thorburn A, Thamm DH, Gustafson DL. Autophagy and cancer therapy. *Mol Pharmacol*. 2014; 85(6):830–8. <https://doi.org/10.1124/mol.114.091850> PMID: 24574520;
18. Bursch W, Ellinger A, Kienzl H, Torok L, Pandey S, Sikorska M, et al. Active cell death induced by the anti-estrogens tamoxifen and ICI 164 384 in human mammary carcinoma cells (MCF-7) in culture: the role of autophagy. *Carcinogenesis*. 1996; 17(8):1595–607. PMID: 8761415.
19. Kim HS, Tian L, Jung M, Choi SK, Sun Y, Kim H, et al. Downregulation of Choline Kinase-Alpha Enhances Autophagy in Tamoxifen-Resistant Breast Cancer Cells. *PLoS One*. 2015; 10(10):e0141110. <https://doi.org/10.1371/journal.pone.0141110> PMID: 26496360;
20. Naressi A, Couturier C, Devos JM, Janssen M, Mangeat C, de Beer R, et al. Java-based graphical user interface for the MRUI quantitation package. *MAGMA*. 2001; 12(2–3):141–52. PMID: 11390270.
21. Tian L, Kim HS, Kim H, Jin X, Jung HS, Park KS, et al. Changes in metabolic markers in insulin-producing beta-cells during hypoxia-induced cell death as studied by NMR metabolomics. *Journal of proteome research*. 2013; 12(8):3738–45. <https://doi.org/10.1021/pr400315e> PMID: 23795807.
22. Thomas C, Gustafsson JA. A CUE hints at tumor resistance. *Nature medicine*. 2011; 17(6):658–60. <https://doi.org/10.1038/nm0611-658> PMID: 21647141.
23. Ring A, Dowsett M. Mechanisms of tamoxifen resistance. *Endocrine-related cancer*. 2004; 11(4):643–58. <https://doi.org/10.1677/erc.1.00776> PMID: 15613444.
24. Thewes V, Simon R, Schroeter P, Schlotter M, Anzeneder T, Buttner R, et al. Reprogramming of the ER α and ER α target gene landscape triggers tamoxifen resistance in breast cancer. *Cancer research*. 2015; 75(4):720–31. <https://doi.org/10.1158/0008-5472.CAN-14-0652> PMID: 25643697.
25. Sanchez-Lopez E, Zimmerman T, Gomez del Pulgar T, Moyer MP, Lacal Sanjuan JC, Cebrian A. Choline kinase inhibition induces exacerbated endoplasmic reticulum stress and triggers apoptosis via CHOP in cancer cells. *Cell Death Dis*. 2013; 4:e933. <https://doi.org/10.1038/cddis.2013.453> PMID: 24287694;
26. Yalcin A, Clem B, Makoni S, Clem A, Nelson K, Thornburg J, et al. Selective inhibition of choline kinase simultaneously attenuates MAPK and PI3K/AKT signaling. *Oncogene*. 2010; 29(1):139–49. <https://doi.org/10.1038/onc.2009.317> PMID: 19855431.
27. Mitsuhashi S, Hatakeyama H, Karahashi M, Koumura T, Nonaka I, Hayashi YK, et al. Muscle choline kinase beta defect causes mitochondrial dysfunction and increased mitophagy. *Hum Mol Genet*. 2011; 20(19):3841–51. <https://doi.org/10.1093/hmg/ddr305> PMID: 21750112;
28. Clem BF, Clem AL, Yalcin A, Goswami U, Arumugam S, Telang S, et al. A novel small molecule antagonist of choline kinase- α that simultaneously suppresses MAPK and PI3K/AKT signaling. *Oncogene*. 2011; 30(30):3370–80. <https://doi.org/10.1038/onc.2011.51> PMID: 21423211;
29. Vogel C, Marcotte EM. Insights into the regulation of protein abundance from proteomic and transcriptomic analyses. *Nat Rev Genet*. 2012; 13(4):227–32. <https://doi.org/10.1038/nrg3185> PMID: 22411467;
30. Fanciulli M, Bruno T, Giovannelli A, Gentile FP, Di Padova M, Rubiu O, et al. Energy metabolism of human LoVo colon carcinoma cells: correlation to drug resistance and influence of lonidamine. *Clin Cancer Res*. 2000; 6(4):1590–7. PMID: 10778993.
31. Zhao Z, Han F, Yang S, Wu J, Zhan W. Oxamate-mediated inhibition of lactate dehydrogenase induces protective autophagy in gastric cancer cells: involvement of the Akt-mTOR signaling pathway. *Cancer letters*. 2015; 358(1):17–26. <https://doi.org/10.1016/j.canlet.2014.11.046> PMID: 25524555.
32. Brisson L, Banski P, Sboarina M, Dethier C, Danhier P, Fontenille MJ, et al. Lactate Dehydrogenase B Controls Lysosome Activity and Autophagy in Cancer. *Cancer Cell*. 2016; 30(3):418–31. <https://doi.org/10.1016/j.ccell.2016.08.005> PMID: 27622334.

33. Martinez-Outschoorn UE, Prisco M, Ertel A, Tsigiros A, Lin Z, Pavlides S, et al. Ketones and lactate increase cancer cell "stemness," driving recurrence, metastasis and poor clinical outcome in breast cancer: achieving personalized medicine via Metabolo-Genomics. *Cell Cycle*. 2011; 10(8):1271–86. <https://doi.org/10.4161/cc.10.8.15330> PMID: 21512313;
34. Jain M, Nilsson R, Sharma S, Madhusudhan N, Kitami T, Souza AL, et al. Metabolite profiling identifies a key role for glycine in rapid cancer cell proliferation. *Science*. 2012; 336(6084):1040–4. <https://doi.org/10.1126/science.1218595> PMID: 22628656;
35. Amelio I, Cutruzzola F, Antonov A, Agostini M, Melino G. Serine and glycine metabolism in cancer. *Trends Biochem Sci*. 2014; 39(4):191–8. <https://doi.org/10.1016/j.tibs.2014.02.004> PMID: 24657017;
36. Locasale JW. Serine, glycine and one-carbon units: cancer metabolism in full circle. *Nat Rev Cancer*. 2013; 13(8):572–83. <https://doi.org/10.1038/nrc3557> PMID: 23822983;
37. van der Vos KE, Coffey PJ. Glutamine metabolism links growth factor signaling to the regulation of autophagy. *Autophagy*. 2012; 8(12):1862–4. <https://doi.org/10.4161/auto.22152> PMID: 22996802;
38. Altman BJ, Stine ZE, Dang CV. From Krebs to clinic: glutamine metabolism to cancer therapy. *Nat Rev Cancer*. 2016; 16(10):619–34. <https://doi.org/10.1038/nrc.2016.71> PMID: 27492215.
39. Ramirez de Molina A, Banez-Coronel M, Gutierrez R, Rodriguez-Gonzalez A, Olmeda D, Megias D, et al. Choline kinase activation is a critical requirement for the proliferation of primary human mammary epithelial cells and breast tumor progression. *Cancer research*. 2004; 64(18):6732–9. <https://doi.org/10.1158/0008-5472.CAN-04-0489> PMID: 15374991.
40. Eliyahu G, Kreizman T, Degani H. Phosphocholine as a biomarker of breast cancer: molecular and biochemical studies. *International journal of cancer Journal international du cancer*. 2007; 120(8):1721–30. <https://doi.org/10.1002/ijc.22293> PMID: 17236204.
41. Stewart DA, Winnike JH, McRitchie SL, Clark RF, Pathmasiri WW, Sumner SJ. Metabolomics Analysis of Hormone-Responsive and Triple-Negative Breast Cancer Cell Responses to Paclitaxel Identify Key Metabolic Differences. *Journal of proteome research*. 2016; 15(9):3225–40. <https://doi.org/10.1021/acs.jproteome.6b00430> PMID: 27447733;
42. Mitsuhashi S, Nishino I. Phospholipid synthetic defect and mitophagy in muscle disease. *Autophagy*. 2011; 7(12):1559–61. <https://doi.org/10.4161/auto.7.12.17925> PMID: 22024749;
43. Mori N, Wildes F, Kakkad S, Jacob D, Solaiyappan M, Glunde K, et al. Choline kinase- α protein and phosphatidylcholine but not phosphocholine are required for breast cancer cell survival. *NMR in biomedicine*. 2015; 28(12):1697–706. <https://doi.org/10.1002/nbm.3429> PMID: 26503172.
44. Glunde K, Jie C, Bhujwalla ZM. Molecular causes of the aberrant choline phospholipid metabolism in breast cancer. *Cancer research*. 2004; 64(12):4270–6. <https://doi.org/10.1158/0008-5472.CAN-03-3829> PMID: 15205341.
45. Jia M, Andreassen T, Jensen L, Bathen TF, Sinha I, Gao H, et al. Estrogen Receptor α Promotes Breast Cancer by Reprogramming Choline Metabolism. *Cancer research*. 2016; 76(19):5634–46. <https://doi.org/10.1158/0008-5472.CAN-15-2910> PMID: 27457520.
46. Ni Chonghaile T, Sarosiek KA, Vo TT, Ryan JA, Tammareddi A, Moore Vdel G, et al. Pretreatment mitochondrial priming correlates with clinical response to cytotoxic chemotherapy. *Science*. 2011; 334(6059):1129–33. <https://doi.org/10.1126/science.1206727> PMID: 22033517;
47. Nazarewicz RR, Zenebe WJ, Parihar A, Larson SK, Alidema E, Choi J, et al. Tamoxifen induces oxidative stress and mitochondrial apoptosis via stimulating mitochondrial nitric oxide synthase. *Cancer research*. 2007; 67(3):1282–90. <https://doi.org/10.1158/0008-5472.CAN-06-3099> PMID: 17283165.
48. Martinez-Outschoorn UE, Goldberg A, Lin Z, Ko YH, Flomenberg N, Wang C, et al. Anti-estrogen resistance in breast cancer is induced by the tumor microenvironment and can be overcome by inhibiting mitochondrial function in epithelial cancer cells. *Cancer Biol Ther*. 2011; 12(10):924–38. <https://doi.org/10.4161/cbt.12.10.17780> PMID: 22041887;
49. Rodriguez-Gonzalez A, Ramirez de Molina A, Banez-Coronel M, Megias D, Lacal JC. Inhibition of choline kinase renders a highly selective cytotoxic effect in tumour cells through a mitochondrial independent mechanism. *Int J Oncol*. 2005; 26(4):999–1008. PMID: 15753995.
50. Raykov Z, Grekova SP, Bour G, Lehn JM, Giese NA, Nicolau C, et al. Myo-inositol trispyrophosphate-mediated hypoxia reversion controls pancreatic cancer in rodents and enhances gemcitabine efficacy. *International journal of cancer Journal international du cancer*. 2014; 134(11):2572–82. <https://doi.org/10.1002/ijc.28597> PMID: 24214898.
51. Criollo A, Maiuri MC, Tasdemir E, Vitale I, Fiebig AA, Andrews D, et al. Regulation of autophagy by the inositol trisphosphate receptor. *Cell Death Differ*. 2007; 14(5):1029–39. <https://doi.org/10.1038/sj.cdd.4402099> PMID: 17256008.

52. Xiao M, Yang H, Xu W, Ma S, Lin H, Zhu H, et al. Inhibition of alpha-KG-dependent histone and DNA demethylases by fumarate and succinate that are accumulated in mutations of FH and SDH tumor suppressors. *Genes Dev.* 2012; 26(12):1326–38. <https://doi.org/10.1101/gad.191056.112> PMID: 22677546;
53. Yang M, Vousden KH. Serine and one-carbon metabolism in cancer. *Nat Rev Cancer.* 2016; 16(10):650–62. <https://doi.org/10.1038/nrc.2016.81> PMID: 27634448.